International Journal of Hydrogen Energy **37**, 7757–7761 (2012)
doi: 10.1016/j.ijhydene.2012.01.141

Visualization of the water distribution in perforated gas diffusion layers by means of synchrotron X-ray radiography

H. Markötter [a)] *, R. Alink [b)], J. Haußmann [c)], K. Dittmann [a)], T. Arlt [a)], F. Wieder [a), e)], C. Tötzke [a), e)], M. Klages [c)], C. Reiter [c)], H. Riesemeier [d)], J. Scholta [c)], D. Gerteisen [b)], J. Banhart [a), e)], I. Manke [a)]

[a)] Helmholtz-Zentrum Berlin (HZB), Hahn-Meitner-Platz 1, 14109 Berlin, Germany
[b)] Fraunhofer Institut für Solare Energiesysteme (ISE), Heidenhofstr. 2, 79110 Freiburg, Germany
[c)] Zentrum für Sonnenenergie- und Wasserstoff-Forschung Baden-Württemberg (ZSW), Helmholtzstraße 8, 89081 Ulm, Germany
[d)] Bundesanstalt für Materialforschung und -prüfung (BAM), Unter den Eichen 87, 12205 Berlin, Germany
[e)] Technische Universität Berlin (TU-Berlin), Straße des 17. Juni 135, 10623 Berlin, Germany

* Corresponding author:
E-mail address: henning.markoetter@helmholtz-berlin.de
Address: Helmholtz-Zentrum Berlin, Hahn-Meitner-Platz 1, 14109 Berlin, Germany
Tel.: +49 30 8062 42826
Fax.: +49 30 8062 43059

Abstract

Perforated gas diffusion layers (GDLs) of polymer electrolyte membrane fuel cells (PEMFCs) were investigated by means of in-situ synchrotron X-ray radiography during operation. We found a strong influence of perforations on the water distribution and transport in the investigated Toray TGP-H090 GDL. The water accumulates mainly around the perforations, while the holes themselves show varying water distributions. Some remain dry, while most of them fill up with liquid water after a certain period or might serve as drainage volume for effective water transport.

1. Introduction

In polymer electrolyte membrane fuel cells (PEMFCs), a well balanced water management is important for high output power, durability and fuel cell stability [1-4]. The gas diffusion layer (GDL) and the adjacent micro-porous layer (MPL) are the key components for water management optimization and are, therefore, in the focus of many recent research studies [4-9]. Kimball et. al. [10] investigated a single perforation in a GDL and the influence on the water distribution.

A few years ago Gerteisen et al. found that perforations in the GDL can lead to a significantly enhanced overall fuel cell performance with a power output gain of up to 20 % under certain operation conditions [11]. In a further publication [12] it was

postulated that the observed performance gain might be related to an in-plane transport of liquid water in the GDL towards the perforation hole, acting as a drain and enabling an easy through-plane water transport.

The liquid water distribution in operated PEM fuel cells can be effectively investigated by neutron radiography, since a high attenuation of neutrons by water comes along with a low attenuation by the cell components [13-17]. Manahan et. al. performed first imaging experiments of the water distribution of perforated GDLs with neutrons [18], showing the perforations to be water pooling locations accompanied with an voltage increase of 6% for current densities lower than 1.4 A/cm². A further publication [19] shows the potential of a 7% voltage increase at 50% rel. humidity.

A much more precise imaging method is synchrotron X-ray radiography. Resolutions up to one µm and a high X-ray flux allow time resolutions down to a few milliseconds and are advantageous for in-situ measurements of water distributions, resolving the pores in the GDL [20, 21]. Here, we present the first high resolution imaging study of the water distribution in perforated GDLs under realistic operating conditions and analyze the reason for the previously found performance increase [11].

2. Fuel cell

2.1 Design

A 100 cm² PEMFC with a threefold serpentine flow field consisting of channels with a 1 mm² cross section separated by 1 mm ribs was adapted to meet the requirements of synchrotron radiography. To allow for sufficient beam transmission and achieve optimal sensitivity to water, bores with a diameter of 10 mm were drilled into the end plates, which correspond to the size of the field of view. While the overall active area is 100 × 100 mm², the field of view allows only for the observation of a selected section of 8.8 × 5.9 mm². Toray TGP-H-090 (280 µm thickness) material, perforated in the visualized area, was employed as GDL at the cathode side, while the anode was equipped with an untreated SGL Sigracet® GDL 25BC. The cell was operated at a temperature of 55 °C and a current density of 0.5 A/cm². The supplied gases had a relative humidity of about 75 %. In order to keep the gas channels free of water and to obtain a better view on the GDL water distribution, a rapid gas stream was chosen for the cathode side with a stoichiometric ratio of $\lambda_C = 4.8$. For the anode side, a ratio of $\lambda_A = 2.8$ was set. This corresponds to an average of 17 m/s air speed on the cathode and 4 m/s hydrogen velocity on the anode side.

2.2 Perforation

A promising concept to enhance liquid water transport in fuel cells is based on the creation of efficient transport paths through the GDL into the channel. A straight forward and practical approach is the realization of drainage channels in the through-plane direction. Perforating of the GDL was carried out by a ND:YAG laser prior to cell assembly. Holes were cut into the GDL by several circular movements of the laser beam. During cutting, argon is blown onto the processed area to prevent oxidation. The holes had a diameter of about 210 µm and were arranged in a square pattern with a hole spacing of 1000 µm. 27 holes were observed in the field of view.

3. Synchrotron radiography setup

The measurements were performed at the tomography station at the BAMline (Bessy II electron storage ring, Helmholtz-Zentrum Berlin, Germany). During these investigations, the fuel cell was mounted in front of a $CdWO_4$ (cadmium wolfram oxide) scintillator screen that converted X-rays into visible light, which was then projected onto a 4008 × 2672 pixel CCD detector (PCO4000). See Fig. 1 for a rough sketch. The field of view was about 8.8 × 5.9 mm² with a pixel size of 2.2 µm. The exposure time was set to 7 s. To achieve optimal image contrast the X-ray energy was set to 15 keV using a double multilayer monochromator that provided an energy resolution of $\Delta E/E \sim 1.5$ %.

All images were normalized with respect to the image of a dry cell in order to extract and quantify the liquid water distribution from the projection images.

4. Results

A radiographic sequence of the cell equipped with a perforated GDL is presented in Fig. 2. Exemplarily it shows the water distribution of a channel section, which comprises four horizontally aligned holes in the perforated GDL. In Fig. 2 a), the positions of the holes as well as the sloped channel walls are sketched.

Subsequent to a current step from 0 to 0.5 A/cm², water is produced in the cell showing up as bright areas all over the image. Liquid product water forms agglomerations in the GDL and the evolution of droplets is observed at the channel walls. Within 10:51 minutes, the GDL areas around the holes constantly fill with liquid water up to a thickness of about 200 µm (see also schematic drawing in Fig. 3 a).

With the assumption that the fiber material itself is uncompressible the total pore volume thickness $\mathbf{V_P}$ can be calculated with the following equation (1):

$$\mathbf{V_P} = \mathbf{d}\,(\mathbf{P} - \mathbf{C}) \tag{1}$$

Where the GDL porosity **P** is 78 %, the initial thickness of the Toray paper **d** is about 280 µm and the GDL compression **C** approximately 20 % in through plane direction. This leads to a maximum liquid water thickness of 162 µm that can be stored inside the cathode GDL. Assuming some water in the anode GDL due to back diffusion, it can be said, that the cathode GDL areas around the holes are almost completely filled with liquid water and remain flooded until the end of the observed operation sequence (30 minutes after the current step).

The filling of the holes themselves shows differing characteristics. Among the 27 investigated holes about 8 (30 %) stay empty throughout operation. The remaining holes fill up with water and remain flooded until the end of the sequence (14 or about 50 %) or fill up and are subsequently emptied at least once (5 or about 20 %).

Examples for this behavior are given with the 4 holes shown in Fig. 2. After 7:21 min of cell operation, hole #1 starts to gather water at the boundary and after 12:08 min the hole itself is completely filled with liquid water. Apparently at the same time, the surrounding area has also reached full liquid water saturation. In almost the same manner the vicinity of hole #3 fills simultaneously with the hole. Both, hole #1 and #3 remain filled during the remaining visualization time.

Hole #2 belongs to the group of perforations which stay clear of water throughout the sequence. However, around this perforation water also agglomerates and reaches saturation in an annular area of the GDL. Right next to the hole water breaks through into the channel, which is indicated by the red arrow in Fig. 2 e). This water break through can be deduced from the water thickness which increases to ~270 µm at this spot and exceeds the maximum water uptake capacity of the GDL. Thus, a water droplet extends into the channel and is later (not shown here) dragged away by a flush of water moving through the channel, resulting in a reduction of thickness to ~180 µm.

At hole #4 the surrounding area has been filled after 10:51 min after which the perforation itself is filled and mostly emptied again within 5 min. The hole might act as a water reservoir connected to an active transport path through the GDL, which causes the observed temporary filling.

According to Fig. 2 f) the water depths of the holes (avg. 300 µm) are higher than those of the surrounding areas (avg. 200 µm). There are different reasons for this. First of all, water inside the GDL can only reside in pore spaces. Taking the porosity of the compressed GDL into account water can only fill 72 % (corresponding to ~162 µm layer thickness) of the compressed GDL volume, whereas it can occupy the whole volume of the hole. Moreover, water inside the holes can eventually pile up and form a meniscus that extends into the channel as sketched in Fig. 3 b).

5. Discussion

The GDL in the close vicinity of the holes acts like a sponge as these areas accumulate augmented water during startup and remain wet throughout operation. This is in line with the findings from Manahan et. al. [18]. It can be assumed that these GDL areas have lost their original hydrophobic characteristics during laser treatment. Since the GDL used does not contain Teflon to increase hydrophobicity, Teflon modification cannot be a reason for the observed hydrophilic behavior. Despite the argon purge during laser perforation residual oxygen remaining on the fiber surface might oxidize the fibers at the high temperatures occurring during cutting and possibly lead to a production of graphite oxide, as assumed in previous work [12]. In some cases the large amount of water around the perforation fills the whole local GDL pore structure. This may block gas transport to the catalyst at such locations. Manahan and Mench [19] already found a performance decrease at higher currents with 300 µm sized perforations, that are showing heavy mass-transport losses at low humidity and even severe performance losses under over-humidified conditions.

Taking into account all 27 perforation holes located in the field of view, strongly varying water distributions were observed inside and around the holes. The differing flooding tendency of the holes indicates the variability of the transport behavior throughout the perforated regions. Small changes in the MPL and GDL pore geometry might result in different local conditions, influence the water distribution and thereby the cell performance. Therefore, the performance gain of perforated GDLs found in in-situ experiments strongly depends on the operating parameters and might also be very sensitive to the conditions during laser perforation [11, 12].

6. Conclusions

We performed a study of water distribution in GDLs of PEM fuel cells with a perforated GDL at the cathode side. We found a strong influence of perforation on the local water distribution and transport. The GDL acts more hydrophilic around the perforation holes, i.e. water preferentially accumulates in these areas, which remain wet all the time during operation. This will block the local gas supply and lead to decreased fuel cell performance.

In general, we found that the filling of the holes themselves shows diverging characteristics and is not individually predictable. Besides variances in the perforation process it might strongly depend on several fuel cell parameters such as current density distribution, temperature distribution and GDL structure just to name a few. The complex behavior should be investigated in further studies, including tomographic investigations allowing for the identification of preferred transport paths in three dimensions. Since the performance increase of perforated GDLs under a small set of operating parameters has already been proven, a thorough understanding of the underlying water transport mechanisms may contribute to significant performance increases with further optimized materials in future.

Acknowledgements

The presented results are part of the activities of the German-Canadian research project 'PEM-Ca-D' financed by the German Federal Ministry of Education and Research (03SF0360B).

References

[1] Vielstich W, Lamm A, Gasteiger HA. Handbook of Fuel Cells – Fundamentals, Technology and Applications. Chichester: John Wiley & Sons; 2003.

[2] Garche J, Dyer CK, Moseley PT, Ogumi Z, Rand DAJ, Scrosati B. Encyclopedia of Electrochemical Power Sources. Amsterdam: Elsevier; 2009. p. 4538.

[3] Carrette L, Friedrich KA, Stimming U. Fuel Cells - Fundamentals and Applications. Fuel Cells. 2001;1:5-39.

[4] Wang C-Y. Fundamental Models for Fuel Cell Engineering. Chem Rev. 2004;104:4727-66.

[5] Manke I, Markötter H, Tötzke C, Kardjilov N, Grothaussmann R, Dawson M, et al. Investigation of energy-relevant materials with synchrotron X-rays and neutrons. Adv Eng Mater. 2011;13:712-29.

[6] Sasabe T, Deevanhxay P, Tsushima S, Hirai S. Soft X-ray visualization of the liquid water transport within the cracks of micro porous layer in PEMFC. Electrochem Commun. 2011;13:638-41.

[7] Thiedmann R, Hartnig C, Manke I, Schmidt V, Lehnert W. Local Structural Characteristics of Pore Space in GDLs of PEM Fuel Cells Based on Geometric 3D Graphs. J Electrochem Soc. 2009;156:B1339-B47.

[8] Benziger J, Nehlsen J, Blackwell D, Brennan T, Itescu J. Water flow in the gas diffusion layer of PEM fuel cells. Journal of Membrane Science. 2005;261:98-106.

[9] Gostick JT, Ioannidis MA, Fowler MW, Pritzker MD. On the role of the microporous layer in PEMFC operation. Electrochem Commun. 2009;11:576-9.

[10] Kimball EE, Benziger JB, Kevrekidis YG. Effects of GDL Structure with an Efficient Approach to the Management of Liquid water in PEM Fuel Cells. Fuel Cells. 2010;10:530-44.
[11] Gerteisen D, Heilmann T, Ziegler C. Enhancing liquid water transport by laser perforation of a GDL in a PEM fuel cell. J Power Sources. 2008;177:348-54.
[12] Alink R, Gerteisen D, Mérida W. Investigating the Water Transport in Porous Media for PEMFCs by Liquid Water Visualization in ESEM. Fuel Cells. 2011;11:481-8.
[13] Schröder A, Wippermann K, Lehnert W, Stolten D, Sanders T, Baumhöfer T, et al. The influence of gas diffusion layer wettability on direct methanol fuel cell performance: A combined local current distribution and high resolution neutron radiography study. J Power Sources. 2010;195:4765-71.
[14] Bellows RJ, Lin MY, Arif M, Thompson AK, Jacobson D. Neutron Imaging Technique for In Situ Measurement of Water Transport Gradients within Nafion in Polymer Electrolyte Fuel Cells. J Electrochem Soc. 1999;146:1099-103.
[15] Satija R, Jacobson DL, Arif M, Werner SA. In situ neutron imaging technique for evaluation of water management systems in operating PEM fuel cells. J Power Sources. 2004;129:238-45.
[16] Hickner MA, Siegel NP, Chen KS, Hussey DS, Jacobson DL, Arif M. In Situ High-Resolution Neutron Radiography of Cross-Sectional Liquid Water Profiles in Proton Exchange Membrane Fuel Cells. J Electrochem Soc. 2008;155:427-34.
[17] Kramer D, Zhang J, Shimoi R, Lehmann E, Wokaun A, Shinohara K, et al. In situ diagnostic of two-phase flow phenomena in polymer electrolyte fuel cells by neutron imaging: Part A. Experimental, data treatment, and quantification. Electrochim Acta. 2005;50:2603-14.
[18] Manahan MP, Hatzell MC, Kumbur EC, Mench MM. Laser perforated fuel cell diffusion media. Part I: Related changes in performance and water content. J Power Sources. 2011;196:5573-82.
[19] Manahan M, Mench M. Increased Performance of PEFCs with Engineered Mass-Transport Pathways. ECS Transactions. 2011;41:569-81.
[20] Manke I, Hartnig C, Grünerbel M, Lehnert W, Kardjilov N, Haibel A, et al. Investigation of water evolution and transport in fuel cells with high resolution synchrotron x-ray radiography. Appl Phys Lett. 2007;90:174105.
[21] Hartnig C, Manke I, Schloesser J, Krüger P, Kuhn R, Riesemeier H, et al. High resolution synchrotron X-ray investigation of carbon dioxide evolution in operating direct methanol fuel cells. Electrochem Commun. 2009;11:1559-62.

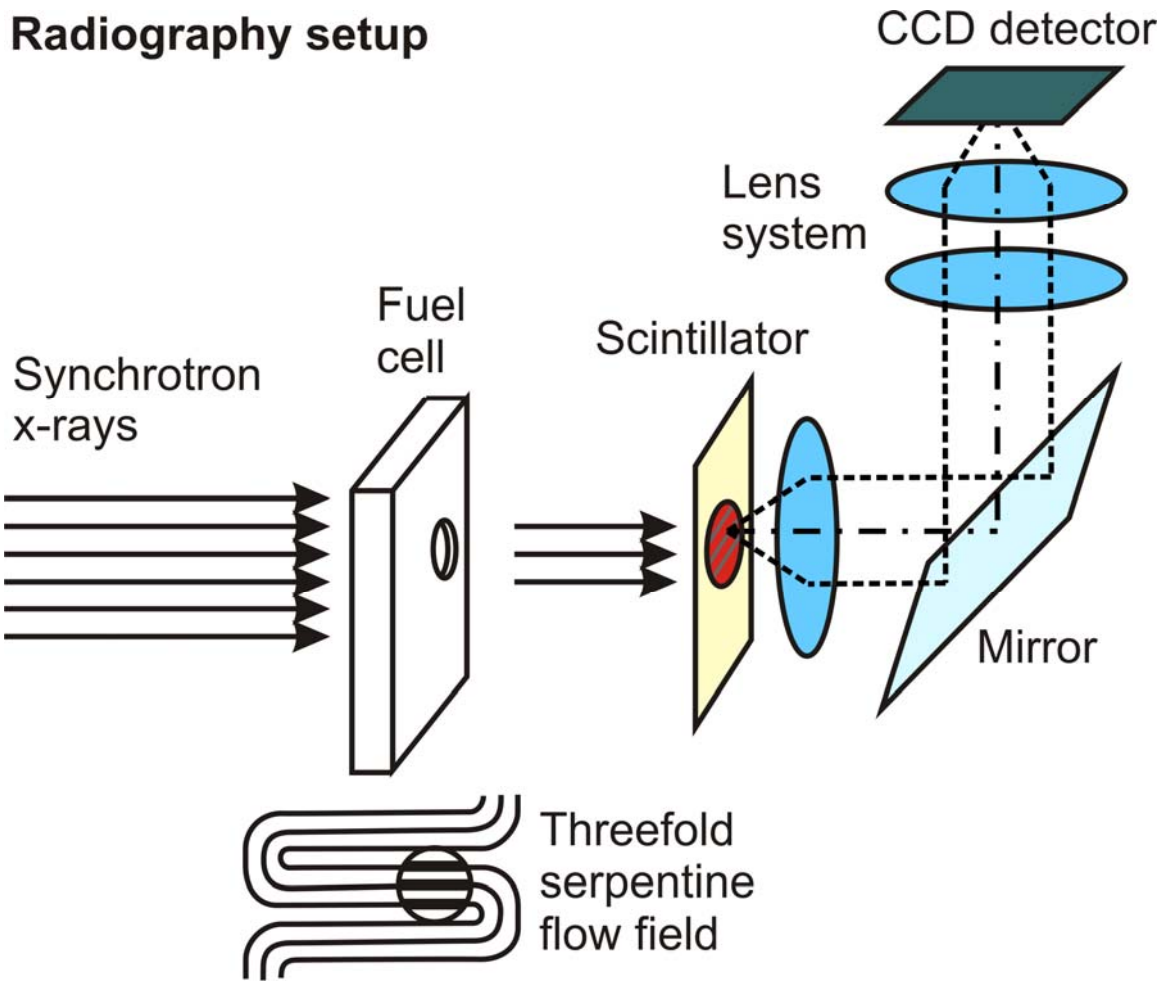

Fig. 1: Radiography setup: The fuel cell is projected in through plane direction onto the scintillator, which is imaged via a mirror onto the CCD to prevent radiation damage of the camera system.

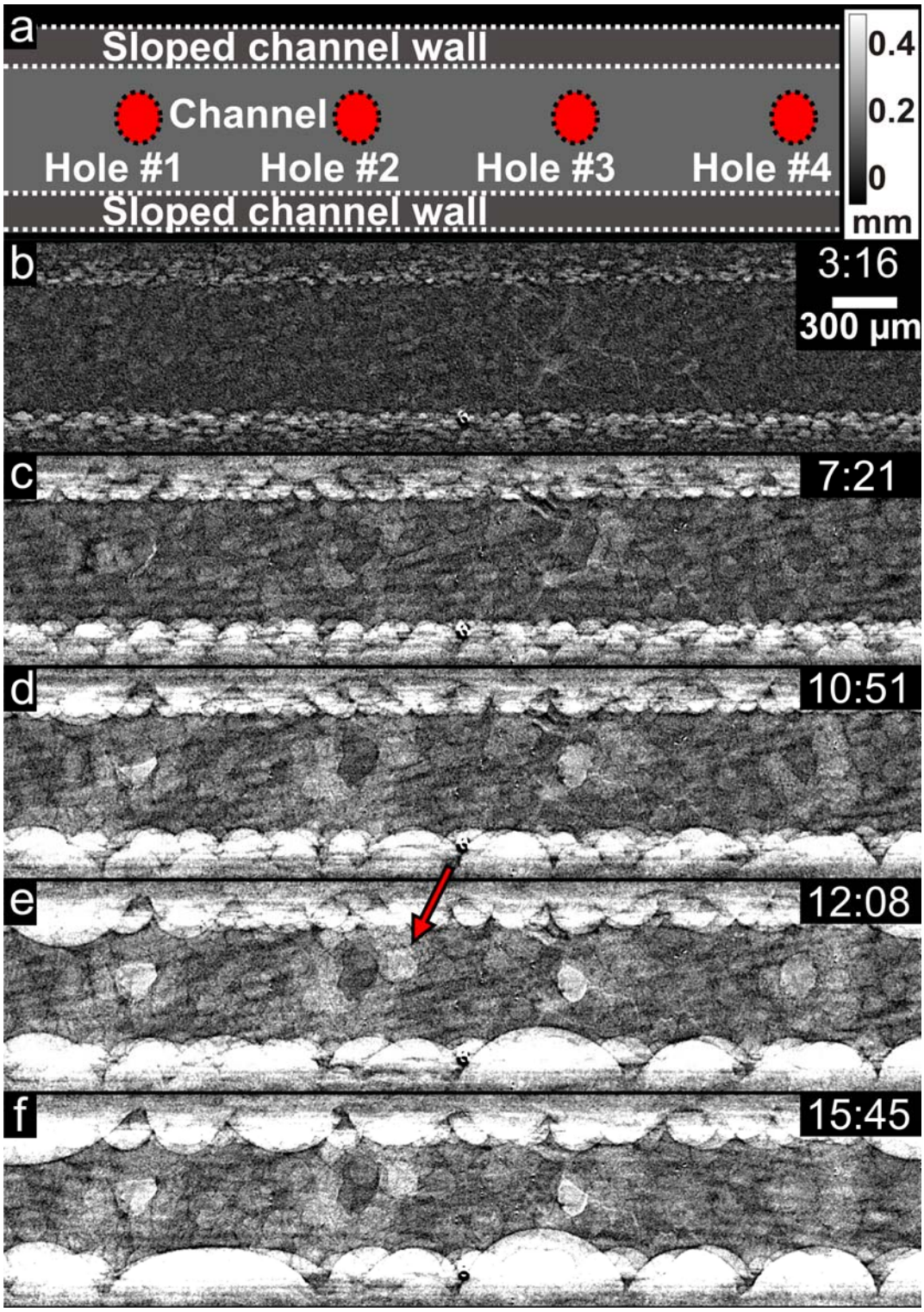

Fig. 2: **a) Drawn position of the cells channel and rib as well as the position of the imaged holes. Cathode gas flow points to the right.**
b) - f) Water distribution at holes of a perforated GDL subsequent to start up from 0 to 0.5 A/cm². The areas around the holes fill up with water as well as most of the holes.

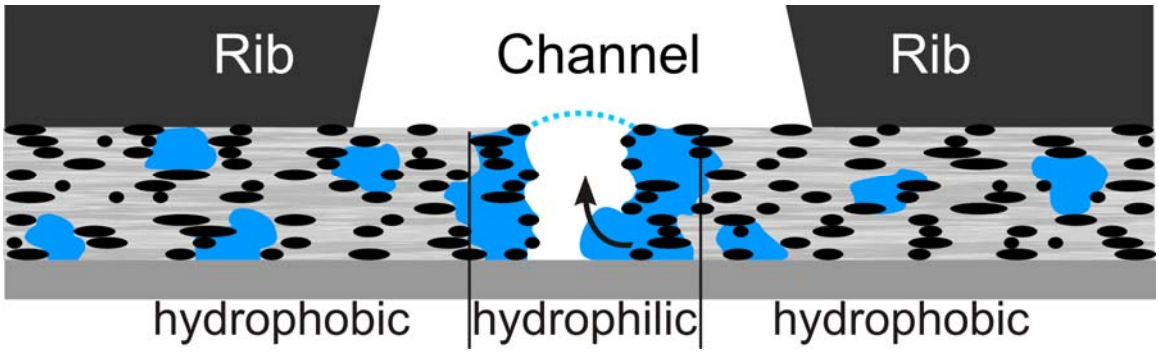

Fig. 3: Sketch of a cut through a perforated GDL. The areas around the perforation holes fill with water, while the holes themselves are not necessary filled.